A NUMERICAL STUDY ON NON-LINEAR AVO INVERSION USING CHAOTIC QUANTUM PARTICLE SWARM OPTIMIZATION

SAM ZANDONG SUN and LIFENG LIU

Laboratory for Integration of Geology & Geophysics, China University of Petroleum, Beijing, P.R. China. szd@cup.edu.cn; liulifeng@cup.edu.cn

(Received October 25, 2013; revised version accepted July 26, 2014)

ABSTRACT

Sun, S.Z. and Liu, L., 2014. A Numerical study on non-linear AVO inversion using chaotic quantum particle swarm optimization. *Journal of Seismic Exploration*, 23: 379-392.

Particle swarm optimization (PSO) is a common method for a non-linear system used in AVO inversion, which is much more advantageous than traditional linear inversion, due to independence of initial model establishment and wavelet estimation, etc. However, the method is prone to fall into local optimum. And it is so easy to be affected by noise interference that fails to tackle the issues of reservoir and fluids in most cases. Based on the method above, a new non-linear AVO inversion method is proposed in this paper, with the employment of chaotic quantum particle swarm optimization (CQPSO) to solve non-linear problems. By comparison with conventional PSO, CQPSO shows more efficient capability, including shorter computation time, higher efficiency for convergence, and global search capability, etc. Due to these characteristics, CQPSO inversion could be used to extract elastic properties directly from the synthetic seismogram, and provide more precise results, especially for density gradients. After the testing with model data and seismic data, the results of CQPSO inversion are all coincident with well data on reservoir properties and fluid content. These coincidences mean confirmed feasibility and effectiveness of the new inversion method.

KEY WORDS: non-linear inversion, particle swarm optimization, global search capability, chaotic mapping, reflection coefficient of density.

INTRODUCTION

Seismic inversion is generally divided into two major categories: pre-stack inversion and post-stack inversion. Pre-stack inversion always maintains the characteristics of seismic reflection amplitude varying with offset, and thus could provide many kinds of elastic properties, such as P-wave reflection coefficient (R_P), S-wave reflection coefficient (R_S), density reflection coefficient

0963-0651/14/$5.00

(R_ρ) and Poisson's ratio. Then the reservoir and fluids could be identified by these properties. Two types of inversion methods are proposed by predecessors from the method implementation: linear inversion and non-linear inversion. They are sometimes both summed up into some extreme values of each objective function. The function of linear inversion always has only one set uncertain values, while the function of non-linear inversion has more.

The essentially process of pre-stack inversion is non-linear, and has more extreme values. However, linear inversion methods, which use the Zoeppritz equation [see eq. (A-1) in the Appendix] and its simplified equations directly, are usually the linearization of non-linear problem, providing an unstable solution, influenced by the initial model (Wang, 2007). On the contrary, non-linear inversion, which needs not any approximation but runs with optimization methods, is a basic way to solve the non-linear problems (Tarantola, 1984; Pratt et al., 1998). Also, non-linear inversion method has other defects, including big workload, long operation time, and low operation efficiency. But non-linear inversion would be the mainstream method in the future, because of its characteristics of fast convergence, global search capability and independence on initial geological model (Kuzma and Rector, 2004; Yang and Yin, 2008; Peng et al., 2008; Yan et al., 2009; Bing et al., 2012).

Particle swarm optimization (PSO) is a common non-linear method used in non-linear AVO inversion, showing advantages of less artificial adjustable parameters, high precision and fast convergence speed. Based on this method, a new non-linear AVO inversion method is proposed in this paper, with an employment of chaotic quantum particle swarm optimization (CQPSO) to solve non-linear problems. The method could be used to correct the faults in PSO inversion, include of easily falling into local optimum and difficultly converging in global space.

BASIC PRINCIPLE OF AVO INVERSION

The kernel of CQPSO inversion is conventional AVO inversion. The Gidlow approximate equation (Gidlow et al., 1992) is employed in CQPSO inversion. Gidlow et al. rearranges the classic equation of Aki and Richards in accordance with the reflection coefficients of P-wave impedance, S-wave impedance and density. The equation is as follows:

$$R_{PP}(\theta) = (1 + \tan^2\theta)R_P - 8(V_S/V_P)^2R_S\sin^2\theta + [4(V_S/V_P)^2\sin^2\theta - \tan^2\theta]R_\rho \quad , \tag{1}$$

where

$$R_P = \tfrac{1}{2}(\Delta V_P\rho/V_P\rho) = \tfrac{1}{2}(\Delta I_P/I_P) \quad ,$$

$$R_S = \tfrac{1}{2}(\Delta V_S\rho/V_S\rho) = \tfrac{1}{2}(\Delta I_S/I_S) \quad ,$$

$$R_\rho = \tfrac{1}{2}(\Delta\rho/\rho) \quad ,$$

and θ is the average angle of incidence angle and transmission angle, R_P is the reflection coefficient of P-wave impedance; R_S is the reflection coefficient of S-wave impedance, R_ρ is the reflection coefficient of density; ΔV_P, ΔV_S, and $\Delta\rho$ are the difference properties of P-wave, S-wave and density respectively of between above interface medium and below interface medium; V_P, V_S and ρ are average properties of P-wave, S-wave and density, respectively, of between above interface medium and below interface medium.

THE PRINCIPLE OF CQPSO

When the ergodic regularity of chaotic mapping is employed into QPSO (see the Appendix), CQPSO is proposed with features of jumping out quickly from local optimum, and keeping the variety of swarm. The basic idea of CQPSO could be expressed by two factors. On the one side, the initialized position of particle in chaotic mapping is employed in CQPSO, ensuring to traverse the entire searching space as much as possible. Not only the randomness would be preserved in the initialization stage of the CQPSO process, but the variety and ergodicity of swarm would be improved in chaotic mapping. On the other side, when quantum particle swarm is evaluated to be fallen into the state of premature convergence in the CQPSO process, the initial particle would be replaced with global extremum particle, and suboptimal particles would be replaced with optimal particles in chaotic sequence. Then, the CQPSO process could jump quickly out of local optimum, and continue the searching process in feasible solution space. As a result, global searching is continued to run.

PROCESS OF CQPSO INVERSION

In eq. (1), the uncertainty of V_S/V_P leads to a non-linear characteristic. Conventional linear inversion method uses certain assumption value, which is obtained from logging data and the initial model of rock physics, to replace the uncertainty of V_S/V_P in eq. (1). Therefore, the AVO relation in eq. (1) is turn to a linear relation in conventional linear inversion process. And the results are strongly dependent on the initial model.

On the other hand, non-linear inversion is performed to work out the non-linear equation by using non-linear method directly. Then the CQPSO inversion is proposed as following Step 1 ~ Step 7 to provide accurate results. And the process diagram is shown in Fig. 1.

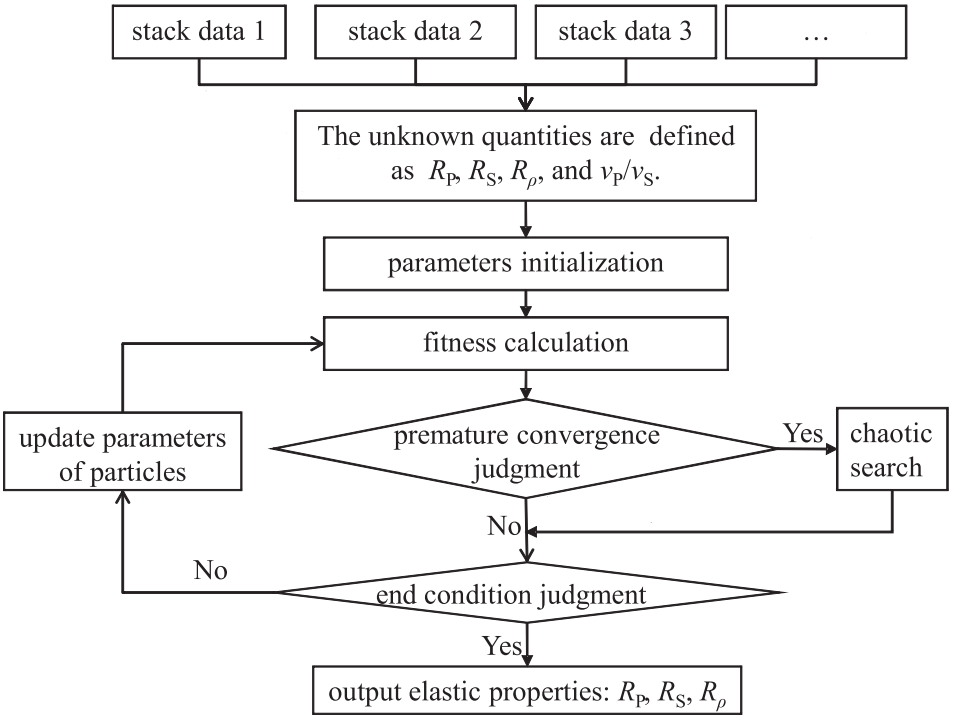

Fig. 1. The process diagram of CQPSO inversion.

Step 1: Stacked seismic data with partial angles, named stack data 1, stack data 2, stack data 3, ..., respectively, according to incident angles, are used as input data in CQPSO inversion. The unknown quantities are R_P, R_S, R_ρ, and V_P/V_S.

Step 2: The total numbers of particles is initialized to M, and the dimension of each particle is 4, including R_P, R_S, R_ρ, and V_P/V_S. The maximum time of iteration process is QPSO_iteration. The maximum time of chaotic sequence is Chaos_iteration. The threshold fitness of ending condition is ε, and the variance threshold fitness of premature convergence is λ. The maximum value and minimum value of quantum particle positions are X_{max} and X_{min}, respectively.

Step 3: A four-dimension random vector generated from [0,1] is used as initial particle. According to Tent mapping (see eq. (A-7) in the Appendix), a Chao_iteration number of random chaotic sequences is generated.

Step 4: M particles are introduced into eq. (1) to calculate the theoretical reflection coefficient of each particle. These coefficients are then introduced into eq. (2), respectively, to evaluate the fitness of each particle, which is considered as the Error E between the theoretical reflection coefficient and the actual reflection coefficient. The smaller is the fitness of the particle, the more accurate to real result. All the particle fitness is then sorted to obtain the individual extremum p_{best} and the global extremum g_{best}.

$$E(t) = \sum_{j=1}^{n} [R_{obs}(\theta_j) - R_{cal}(\theta_j)]^2 \quad , \tag{2}$$

where R_{obs} is the reflection coefficient extracted from gathers; R_{cal} is the reflection coefficient calculated by eq. (1); n is the number of partial-angle-stacked data, usually 3 or 4; θ_j is the j-th average angle of incidence angle and transmission angle; i represents the i-th particle.

Step 5: Premature convergence judgment. If the variance of global fitness, calculated by eq. (3), is smaller than λ, turn to Step 6, or turn to Step 7.

$$\sigma^2 = (1/M) \sum_{j=1}^{n} [(f_i - f_{avg})/f]^2 \quad . \tag{3}$$

Step 6: Chaotic variation. The global extremum g_{best} is chosen as the initial particle. According to the Tent mapping, certain percentages of most optimal mapping particles are selected to update the raw particles with suboptimal behaviour.

Step 7: Ending condition judgment. If the fitness of the global extremum g_{best} is smaller than the variance threshold fitness λ, exit; and if the number of iteration time reaches the maximum time Chaos_iteration, exit. Or, update all particles by using eqs. (A-3)~(A-5) in the Appendix, and turn to Step 4. Reiterate until the global optimal value is found out.

MODEL DATA FOR TESTING

A forward modeling is proposed to verify the availability of CQPSO inversion. The model is generated by logs of high-yield drilling in the Tarim basin. To correspond with seismics, the logs of P-wave, S-wave and density are converted from depth domain to time domain. And the logs are sampled with a 2 ms interval, the same as the interval of seismic data (Fig. 2). The gathers data of the model is generated by using complete Zoeppritz equation (see eq. (A-1) in the Appendix) with a 40 Hz Ricker wavelet (Fig. 3).

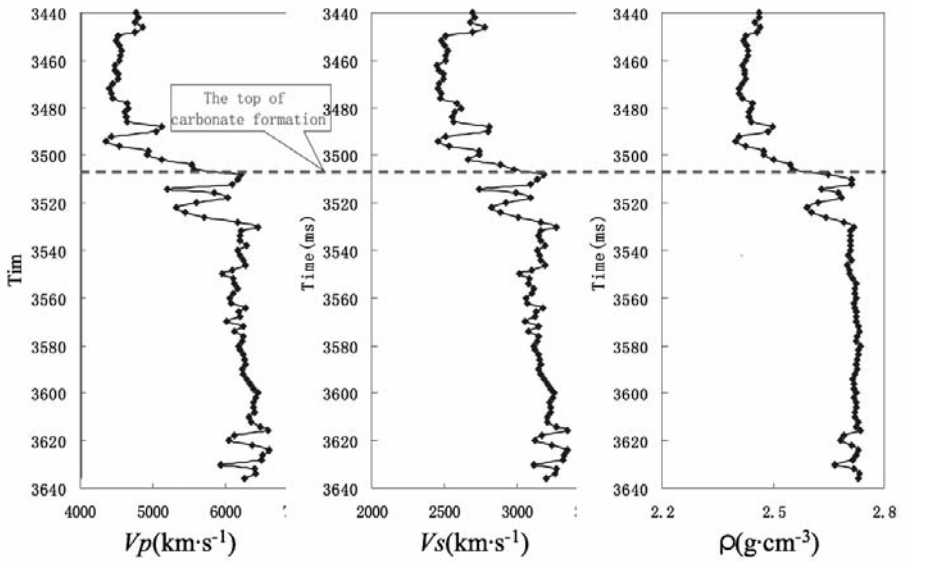

Fig. 2. The model is generated by logs of a high-yield drilling in Tarim basin. To correspond with seismic, the logs are converted from depth domain to time domain with 2 ms sample interval.

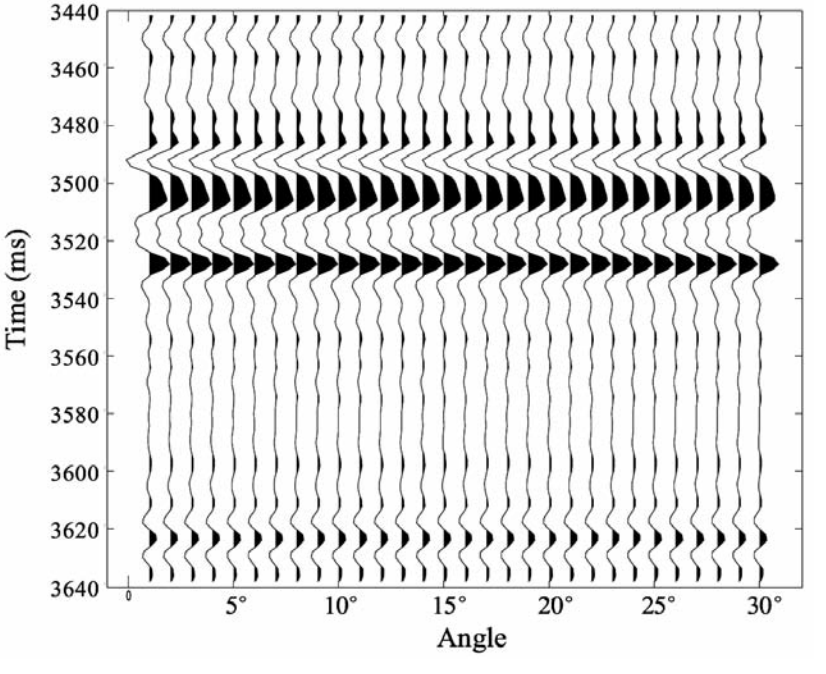

Fig. 3. The gathers data of model is generated by using complete Zoeppritz equation. The maximum incident angle is 30°. The convolution is performed with a 40 Hz Ricker wavelet.

PSO INVERSION FOR MODEL GATHERS DATA

Model gathers data is used in PSO inversion to achieve elastic properties. The parameters of PSO inversion is as follows: The total number of particle swarm is 30. The maximum iteration time is 100000. The accelerating factors c_1 and c_2 are both 2.04 (see eq. (A-2) in the Appendix). The initial inertia factor ω_{max} is 0.9. When the iteration time reaches the maximum time, the inertial factor ω_{max} is set at 0.5. The search range of R_P, R_S, R_ρ and V_P/V_S are $(-0.1 \sim 0.1)$, $(-0.1 \sim 0.1)$, $(-0.05 \sim 0.05)$ and $(0.4 \sim 0.7)$, respectively. The ending condition of error threshold ε is 10^{-11}.

The results of PSO inversion are diagramed in Fig. 4. The logs are reflection coefficient of R_P, R_S, and R_ρ. Blue dot line represents the properties from drilling logs, while pink dot line represents corresponding properties from PSO inversion result. R_P result is coincidence with R_P log in the left part of Fig. 4. And R_S result is also coincidence with R_S log in the central part of Fig. 4, with a slightly unfitness.

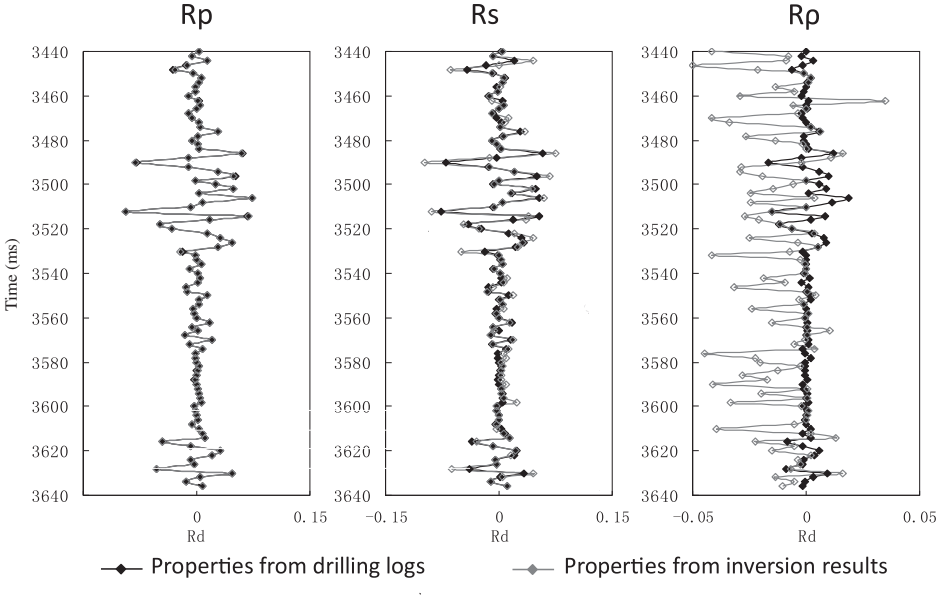

Fig. 4. The properties of drilling logs and PSO inversion results are diagramed with dot lines. The logs are reflection coefficient of R_P, R_S, and R_ρ, respectively. Blue dot line represents the properties from drilling logs, while pink dot line represents corresponding properties from PSO inversion result.

However, R_ρ result is incidence with R_ρ log in the right part of Fig. 4. Actually, R_ρ result is more dependent on the large incident data in seismic gathers, and always shows a high accurate requirement because of the small coefficient value in eq. (7). This incidence means that PSO inversion is not accurate enough to provide benefit R_ρ result.

CQPSO INVERSION FOR MODEL GATHERS DATA

Model gathers data is also used in CQPSO inversion to achieve elastic properties. The corresponding parameters of CQPSO inversion is the same as in PSO inversion. To the difference, the maximum iteration time is 100, and the iteration time of chaotic mapping is 100,000.

The results of CQPSO inversion are diagramed in Fig. 5. As a same result, the logs are also reflection coefficient of R_P, R_S, and R_ρ. It shows a high coincidence in respective comparison of three properties between drilling logs and inversion results. It is obvious that R_ρ result has been improved to be fit with R_ρ log in the right part of Fig. 5. It means that CQPSO inversion is more accurate to provide benefit R_ρ result than PSO inversion. The high efficient global search capability of CQPSO makes the greatest contribution to improve the accuracy.

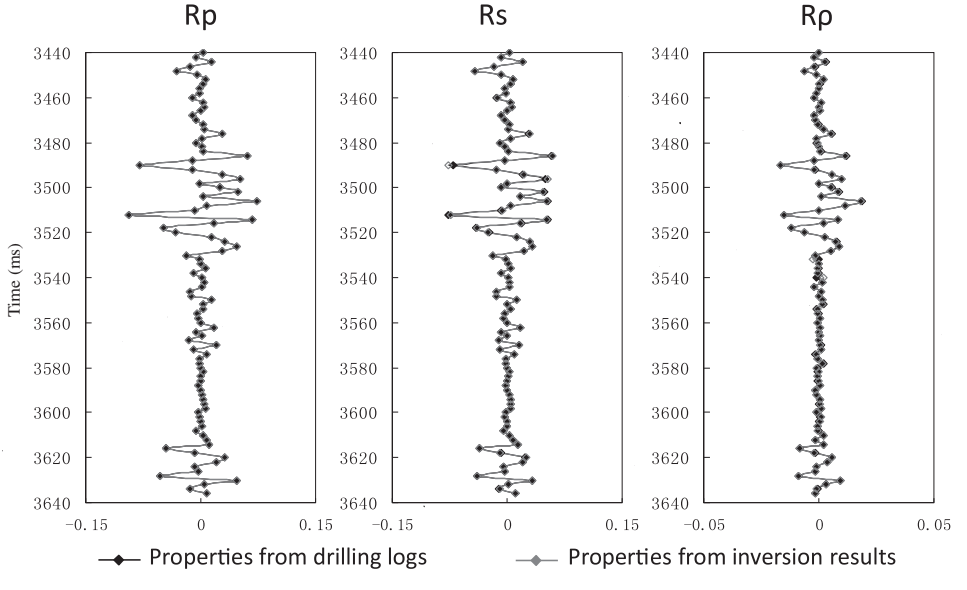

Fig. 5. The properties of drilling logs and CQPSO inversion results are diagramed with dot lines. The properties of logs are the same as in Fig. 4. It is obvious that R_ρ result has been improved to be fit with R_ρ log. It means that CQPSO inversion is more accurate to provide benefit R_ρ result than PSO inversion in Fig. 4.

Practical industry application needs a non-linear inversion with a fast convergence rate, and a high operation speed. Fitness and iteration times are two criterions of process efficiency. Two comparisons of fitness (Step 4) and iteration times (Step 7) between PSO inversion and CQPSO inversion are employed and shown in Fig. 6. The 99 samples are used to test the process of two inversions. In PSO inversion, only 20 samples have available a fitness less than threshold ε, when the iteration time is less than 100,000. And another 79 samples do not have the fitness available. For the whole PSO inversion process,

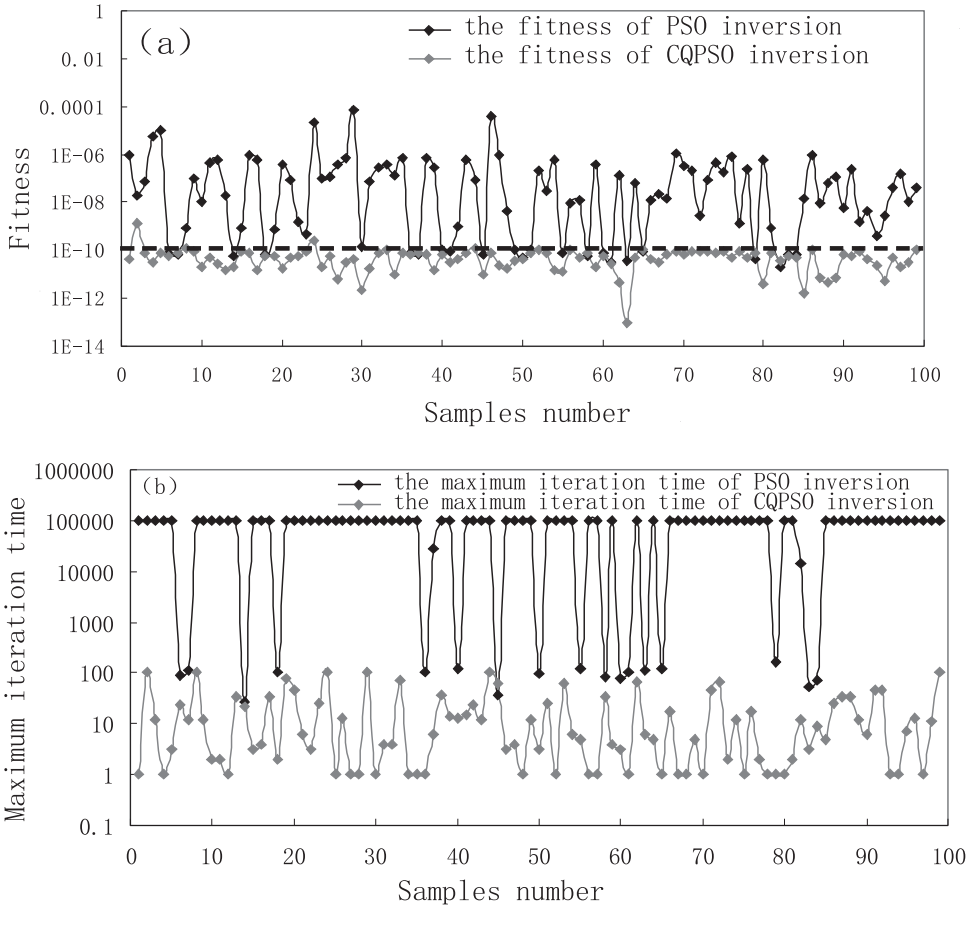

Fig. 6. The results of two comparisons are shown for fitness (a) and maximum iteration time (b) between PSO inversion and CQPSO inversion. The available converged samples in CQPSO inversion are more than that in PSO inversion. While the iteration time in CQPSO inversion are less than that in PSO inversion.

the convergence rate is 20.2%, and the process time is 422 s. In CQPSO inversion, 26 samples have the available fitness in the initial stage. And 56 samples get the available fitness in the stage of less than 10 iteration times. And only 5 samples could not get the available fitness. For the whole CQPSO inversion process, the convergence rate is 94.9%, and the process time is rarely 21 s. Although the chaotic mapping process is added in CQPSO inversion process with a result of increasing extra process time, the global optimization capability has greatly improved the operation speed of CQPSO inversion. With chaotic mapping, the global extremum particle could be found out in a few iteration times. As a result, the process time of CQPSO is obviously cut down to 21 s. Although it still has a larger process time than the linear inversion, the non-linear inversion has been accepted by the practical application, through the measurement of parallel algorithm.

CASE STUDY

CQPSO inversion is employed in X area in Tarim basin to analyze its effectiveness. The target in X area is weathering crust karst reservoirs in carbonate layers of Ordovician. These reservoirs are always linked to bead-like reflection in seismic profiles. In order to identify the lithology, reservoir properties and fluids, AVO inversion is needed to be employed.

Four wells with different reservoir properties and different yield are sampled in this paper. And the results of CQPSO inversion around every well are shown and compared with each other. A few profiles of seismic data and inversion results through wells are shown in Fig. 7. As a matter of fact, well X1 and well X2 have the same financial yield in formation test. But well X1 has great yield in production, while well X2 has a bad yield. Well X3 and its sidetracked hole are all water yield in formation test. And well X4 has a mud filled reservoir, and none yield of a dry hole.

The profiles of inversion properties show some low noise and high quality result data of inversion. Properties values are clear enough to be used to identify lithology, reservoir properties and fluids. R_P could express a great sensitiveness to fracture-cavity carbonate reservoir (Han et al., 2013). Actually, other than the reservoir in well X4 is filled with mudstone, reservoirs in other three wells are all good quality. And the value of R_P data related to well X4 is small, while the values of R_P data related to others wells are big. The values of R_P data related to reservoirs are clear enough to be used to identify carbonate reservoir.

R_ρ is always difficult to be accurately gained in common AVO inversion because of the poor quality of large incident gather data. But CQPSO inversion could be improved to provide accurate R_ρ data by integrated the method of CQPSO. The availability of R_ρ data is always verified by comparison with gas

saturation in reservoir. Research has disclosed an approximate linear relationship between density and gas saturation (Wang, 2005; Chen, 2007). When the gas saturation increases, the density decreases. There is only well X1 with high gas saturation in four wells according to the production data. And only well X1 has a strong amplitude reflection in R_ρ data. That means that R_ρ data of CQPSO inversion is clear enough to be used to identify high yield wells in X area.

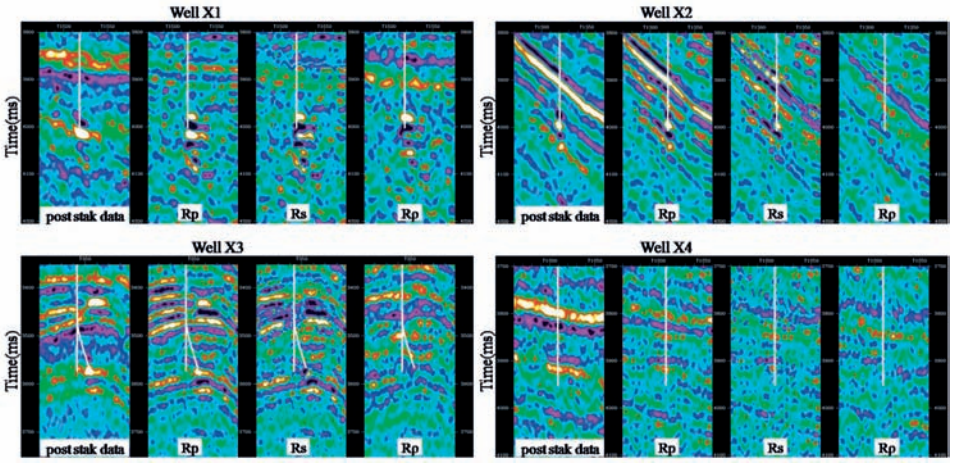

Fig. 7. CQPSO inversion results are shown in short profiles through four typical wells respectively.

CONCLUSIONS

The erdogic feature of chaotic mapping is used into normal PSO algorithm to improve its capability of global optimization. With chaotic mapping, CQPSO could quickly jump out of local optimum, and could avoid falling into the premature convergence. Furthermore, CQPSO could have the qualities of preserved swarm variety and improved searching efficiency.

The process of CQPSO inversion is established to achieve good quality and accurate results. By comparison with conventional PSO, CQPSO has more efficient capability include of shorter operation time, higher efficiency convergence, and global search capability, etc. Due to these available characteristics, CQPSO inversion could be used to extra elastic properties directly from the synthetic seismogram, and provide more precision results, especially for reflection coefficient of density. After the testing with model data and the case study with seismic data, the results of CQPSO inversion are all coincident with drilling data in reservoir properties and fluid enrichment.

ACKNOWLEDGEMENTS

The authors thank the National Basic Research Program of China (Grant No. 2011CB201103), the National Science and Technology Major Project (Grant No. 2011ZX05004003), the National Youth Science Fund Project (41204093) and the Science Foundation of China University of Petroleum-Beijing (KYJJ2012-05-03) for financial support. We would like to thank Tarim Oilfield Co., CNPC for providing the field seismic data.

REFERENCES

Bing, P.P, Cao, S.Y. and Lu, J.T., 2012. Non-linear AVO inversion based on support vector machine. Chin. J. Geophys., 55: 1025-1032 (in Chinese).

Chen, J., 2007. Study of Three-term AVO Inversion Method. Ph.D. Thesis, China Univ. of Petroleum, Dongying (in Chinese).

Fang, W., Sun, J., Xie, Z. and Xu, W., 2010. Convergence analysis of quantum-behaved particle swarm optimization algorithm and study on its control parameter. Acta Phys. Sin., 59: 3686-3693 (in Chinese).

Gidlow, P.M., Smith, G.C. and Vail, P.J., 1992. Hydrocarbon detection using fluid factor traces. Joint SEG/EAEG Summer Res. Worksh., Technical Program and Abstr.: 78-89.

Han., J., Sun, Z., Zhang, X., Zhang, Y., Chen, J., Pan, Y., Liu, X. and Zhao, H., 2013. Integrated identification for complex reservoir based on pure P-wave data and post-stack data. Expanded Abstr., 83rd Ann. Internat. SEG Mtg., Houston.

Kennedy, J. and Eberhart, R., 1995. Particle swarm optimization. Proc. IEEE Internat. Conf. on Neural Networks, Perth, Australia: 1942-1948.

Kuzma, H.A. and Rector, J.W., 2004. Non-linear AVO inversion using support vector machines. Expanded Abstr., 74th Ann. Internat. SEG Mtg., Denver.

Lu, H., 2006. A new optimization algorithm based on chaos. Zhejiang Univ. Science A, 7: 539-542.

Peng, Z., Li, Y., Wei, W., He, Z. and Li, D., 2008. Nonlinear AVO inversion using particle filter. Chin. J. Geophys., 51: 1218-1225 (in Chinese).

Pratt, R.G., Shin, C.S., Hicks, G.J., 1998. Gauss-Newton and full Newton method in frequency-space seismic waveform inversion. Geophys. J. Int., 133: 341-362.

Shan, L., Qiang, H., Li, J. and Wang, Z., 2005. Chaotic optimization algorithm based on Tent map. Control and Decision, 20: 179-182 (in Chinese).

Sun. J., Xu. W.B. and Feng, B., 2004. A global search strategy of quantum-behaved particle swarm optimization. Proc. IEEE Conf. on Cybernetics and Intelligent Systems, Singapore: 111-116.

Tarantola, A., 1984. Inversion of seismic reflection data in the acoustic approximation. Geophysics, 49: 1259-1266.

Tavazoei, M.S. and Haeri, M., 2007. An optimization algorithm based on chaotic behavior and fractal nature. J. Computat. Appl. Mathemat., 206: 1070-1081.

Wang, S., 2005. Elastic properties of gas-bearing strata and seismic response. Oil Gas Geol., 26: 730-735 (in Chinese).

Wang, J., 2007. Lecture on non-linear inverse methods in geophysics. (I): Introduction to geophysical inverse problems. Chin. J. Engin. Geophys., 4: 1-3 (in Chinese).

Yan, Z., Gu, H. and Zhao, X., 2009. Non-linear AVO inversion based on ant colony algorithm. OGP, 44: 700-702 (in Chinese).

Yang, P. and Yin, X., 2008. Non-linear quadratic programming Bayesian prestack inversion. Chin. J. Geophys., 51: 1876-1882 (in Chinese).

APPENDIX

ZOEPPRITZ EQUATION

$$\begin{bmatrix} \sin i_1 & \cos j_1 & -\sin i_1 & \cos j_2 \\ \cos i_1 & -\sin j_1 & \cos j_2 & \sin j_2 \\ \sin 2i_1 & \frac{\alpha_1}{\beta_1}\cos 2j_1 & \frac{\rho_2\beta_2^2\alpha_1}{\rho_1\beta_1^2\alpha_2}\sin 2i_2 & \frac{\rho_2\beta_2\alpha_1}{\rho_1\beta_1^2}\cos 2j_2 \\ \cos 2j_1 & -\frac{\beta_1}{\alpha_1}\sin 2j_1 & -\frac{\rho_2\alpha_2}{\rho_1\alpha_1}\cos 2j_2 & -\frac{\rho_2\beta_2}{\rho_1\alpha_1}\sin 2j_2 \end{bmatrix} \begin{bmatrix} R_{PP} \\ R_{PS} \\ T_{PP} \\ T_{PS} \end{bmatrix} = \begin{bmatrix} -\sin i_1 \\ \cos i_1 \\ \sin 2i_1 \\ -\cos 2j_1 \end{bmatrix}, \quad \text{(A-1)}$$

where R_{PP} is the reflection coefficient of the P-wave; R_{PS} is the reflection coefficient of the S-wave; T_{PP} is the transmission coefficient of the P-wave; T_{PS} is the transmission coefficient of the S-wave; α_1, β_1, ρ_1, α_2, β_2 and ρ_2 are the P-wave velocity, S-wave velocity and density of the media 1 and media 2, which are closely adjacent and different from a reflection interface; i_1 is the incident angle; i_2 is the reflection angle; i_2 and j_2 are transmission angles.

The principle of the family of Particle Swarm Optimization methods

PSO

Particle swarm optimization (PSO) was first proposed by Dr. Eberhart and Dr. Kennedy in 1995, inspired by feeding behavior of birds and fish (Kennedy and Eberhart, 1995). By the sharing information and multiple iterations in whole swarm, PSO shows its advantage of global search method. However, the convergence process in PSO goes easily into local optimum to ending process incorrectness. As a result, PSO is not a global optimization algorithm, and could not ensure to find out the global optimal solutions.

$$V_i^{k+1} = \omega V_i^k + c_1 r_1 (p_{best} - X_i^k) + c_2 r_2 (g_{best} - X_i^k) \quad , \quad \text{(A-2)}$$

$$X_i^{k+1} = X_i^k + V_i^{k+1} \quad , \quad \text{(A-3)}$$

where k is the iteration time; c_1 and c_2 are constant values, which are called acceleration factors. c_1 and c_2 represent the alteration speeds from the current particle values to p_{best} and g_{best}, respectively; ω is the inertial factor, which represents the influence weight from current speed to its next generation; r_1 and r_2 are random numbers in [0,1]; V_i and X_i represent particle speed and position, respectively.

QPSO

In order to improve the global search capability of PSO, Sun et al. (2004) proposed a method of quantum particle swarm optimization (QPSO). In QPSO, particle movement is regarded as a quantum behavior, which means an uncertain trajectory and an arbitrary position in feasible solution space with a certain probability. The global optimization capability of QPSO is far stronger than the one of PSO (Fang, 2010). However, QPSO could not overcome the inherent shortcoming of premature convergence, like other intelligent swarm optimization. In QPSO, all particles are concentrated into a small space, with an almost zero velocity. And particles could not be globally searched in feasible solution space. As a result, QPSO could fall into a state of premature convergence, where QPSO could put all particles together in a later stage, because of its particle memorability and extremum convergence.

$$m_{best} = (1/M)\sum_{i=1}^{M} X_i^k = [(1/M)\sum_{i=1}^{M} X_{i1}^k,(1/M)\sum_{i=1}^{M} X_{i2}^k,\ldots,(1/M)\sum_{i=1}^{M} X_{id}^k] \quad , \qquad \text{(A-4)}$$

$$p_i = \varphi \cdot p_{best} + (1 - \varphi)\cdot g_{best}, \varphi = r_{nad} \quad , \qquad \text{(A-5)}$$

$$X_i^{k+1} = p_i \pm \alpha \cdot |m_{best} - X_i^k| \cdot \ln(1/\mu) \quad , \qquad \text{(A-6)}$$

where m_{best} represents the average optimal position of all particles; φ and μ are random numbers, evenly distributed in [0,1]; α is shrinkage-expansion coefficient, which is used to control the convergence speed; X_i is the position of the i-th particle.

Chaotic mapping

Chaos is a kind of common phenomenon in the evolution of a non-linear system. By using some simple deterministic rules, it could provide a complex long term but not fixed cycle behaviour, which is sensitive to initial conditions. It has some features included of regularity, randomness and ergodicity. And it could traverse all possible states non-repeatedly in a certain space according to its own regularity (Lu, 2006; Tavazoei and Haeri, 2007).

Tent mapping is one of rules which are used to generate chaotic data. It has some advantages of simple structure, good uniformity traversal, and fast iterative speed (Shan et al., 2005).

$$x_{n+1} = \begin{cases} 2x_n & , \quad 0 \le x_n \le 0.5 \\ 2(1 - x_n) & , \quad 0.5 \le x_n \le 1 \end{cases} \quad , \text{ where } n = 1, 2, 3, \ldots \text{(A-7)}$$